

Meyer-Neldel-like manifestation of the quantum confinement effect in solid ensembles of semiconductor quantum dots

I. Balberg, E. Savir, and Y. Dover

The Racah Institute of Physics, The Hebrew University, Jerusalem 91904, Israel

O. Portillo Moreno and R. Lozada-Morales

FCFM, Benemerita Universidad de Puebla 72570, Puebla, Mexico

O. Zelaya-Angel

Department of Physics, CINVESTAV-IPN, P.O. Box 14-470, Distrito Federal de Mexico 07360, Mexico

(Received 11 January 2007; published 3 April 2007)

We report clear crystallite size dependencies of the transport and phototransport properties in solid-state ensembles of semiconductor quantum dots. By finding a Meyer-Neldel-like behavior for the former and by comparing the experimental results with computer simulations for the latter, we show that the above dependencies are associated with the quantum confined induced variation of the band gap in the individual dots. These findings go beyond the available knowledge of interparticle conduction mechanisms by providing a basis for the corresponding physical statistics of such quantum dot ensembles.

DOI: [10.1103/PhysRevB.75.153301](https://doi.org/10.1103/PhysRevB.75.153301)

PACS number(s): 73.63.Kv, 73.22.-f, 73.50.Gr, 73.61.Ga

While the single semiconductor quantum dot is relatively well understood,¹⁻⁴ the understanding of the physical properties⁵⁻⁹ of dense ensembles of quantum dots (QDs) is still at a rudimentary level. In particular, while considerable advances in the evaluation of the optical properties⁶⁻⁸ and in the interdot conduction mechanisms^{5,9} in such ensembles have been reported, no correlation was made between their macroscopic, disordered-semiconductorlike transport and phototransport properties,^{5,9-17} and the quantum confinement induced level shifts in the corresponding individual nanocrystallites (ncs). In this Brief Report, we report such correlations for a prototype of these ensembles and show that these correlations result primarily from the corresponding relative shift between the edge of the ensemble's conducting miniband and the Fermi level of the macroscopic ensemble. Our study then goes beyond all previous studies that were concerned essentially with the intercrystallite conduction mechanism⁹ and not with the statistical physics, i.e., the carrier concentration aspect of the transport in these ensembles.

To illustrate the limited information available for solid state ensembles of semiconductor QDs, let us consider first the fundamental property of the conductivity activation energy E_a that is defined by

$$\sigma = \sigma_0 \exp(-E_a/kT), \quad (1)$$

where σ is the measured conductivity in the dark, σ_0 is the fitted conductivity prefactor, and kT is the thermal energy. As far as we know, models that correlate the value of E_a and the ncs diameter, d , have been proposed previously *only* for porous silicon.¹⁰ In the latter system, however, the involvement of the silicon disordered tissue that encapsulates the crystallites¹¹ and the Coulomb blockade there¹² makes the interpretation¹⁰ of the corresponding electrical transport observations quite indirect. In contrast, in the system of CdSe ncs which is the best representative system of semiconductor quantum dots,² the ncs (and, in particular, the value of d) are

usually^{2,6,13} well characterized (see below) and the geometrical connectivity of the system is simple.⁵

Considering the fact that CdSe QDs serve as a prototype of quantum dot systems^{1,2,8} and that data on these and other systems can be found in the literature¹⁻⁹ let us review briefly in this Brief Report only the information concerning the $E_a(d)$ dependence in ensembles of such dots. Closely packed CdSe ncs that are separated from each other by 1-nm-thick ligands yielded⁵ E_a values in the 0.1–0.2 eV range, but the scattering in those data did not allow the authors to derive a clear correlation between these values and the values of d . This was also the case with various solid (physically deposited) systems of CdSe ncs.¹⁴⁻¹⁶ A clearer correlation was found, however, in films prepared by chemical-bath deposition¹⁷ but, in one case, these results were attributed to doping effects at the grain boundaries and, in another, the relation between the E_a values and the quantum confinement has not been discussed. In all the above studies, the values of σ_0 have not been reported. However, noting the results of Ref. 17, we adopted a similar chemical-bath deposition technique¹⁸ for our present study of the macroscopic transport properties. In particular, using undoped films of the same thickness (200 nm) has enabled us to attribute the observed E_a and σ_0 values more directly to the d values in our ncs that are in the quantum confinement regime ($d < 11.2$ nm) of CdSe.^{1,2} The interpretation that we suggest for the corresponding dependencies follows the self-consistent picture that we found here between the dark and the phototransport properties.

We have previously characterized the microstructure of our deposited films and their optical transmission.^{18,19} The size distribution of the crystallites at a given sample was found to be centered around a diameter d with a distribution width of about $d/5$. The d values, in the range of 7.5–12.5 nm, were determined by the temperature of the chemical solution used in the deposition process.¹⁸ Our transport and phototransport measurements have been car-

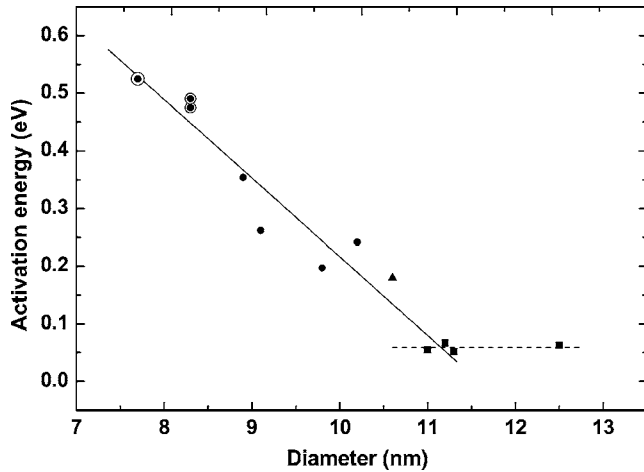


FIG. 1. The observed dependence of the dark conductivity activation energy on the mean crystallites diameter in our corresponding solid-state ensembles of CdSe quantum dots. The lines shown are guides to the eye.

ried out in the coplanar configurations that have been described previously.^{11,20} The optical transmission spectra that we found were very similar to those found⁸ for closely packed ensembles of CdSe quantum dots and they have shown¹⁸ that for the $7.5 \leq d \leq 10.5$ nm range, the change in the optical gap ΔE_g is about 0.3 eV.

Our previously presented typical $\sigma(T)$ dependencies have clearly shown¹⁹ two types of behaviors that are easily correlated with two types of samples,¹⁸ those on which we could measure the electrical conductivity only above relatively high (about 200 K) temperatures and those on which we could measure the conductivity down to the liquid N₂ temperature. Following our previous x-ray data,¹⁸ we know that the samples with $d < 10.5$ nm consist only of hexagonal-wurtzite (HW) crystallites (circles in Figs. 1–3), while samples with $d > 11$ nm consist only of cubic zinc-blende (ZB) crystallites (squares in Figs. 1–3). An intermediate case of a sample with $d = 10.7$ nm (a triangle in Figs. 1–3) is a mixture of the two phases.

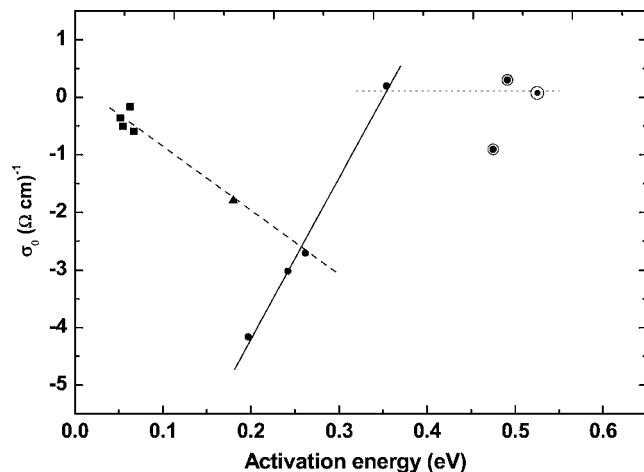


FIG. 2. A Meyer-Neldel-like plot of the dark conductivity prefactor as a function of the activation energies given in Fig. 1 for the three crystallite-size regimes studied in the present work.

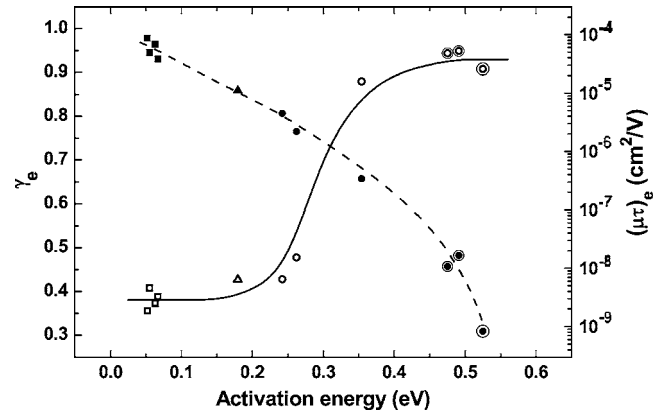


FIG. 3. The measured dependence of the electron's mobility-lifetime product (dashed curve) and the corresponding light intensity exponent (solid curve) on the measured conductivity activation energy in the series of the studied ensembles (i.e., on the crystallites size as given in Fig. 1) at 250 K. The curves shown are guides to the eye.

Analyzing our $\sigma(T)$ data¹⁹ according to the parameters of the Arrhenius plot [Eq. (1)] in the 200–300 K range yielded the $E_a(d)$ dependence that is shown in Fig. 1. We see first a clear transition at $d \approx 11$ nm, which corresponds well to the transition from the HW-type to the ZB-type samples. The scattering in the data does not allow the derivation of an exact functional dependence of E_a on d but the strong monotonic decrease of E_a with increasing d , within the samples of the HW phase, is clear, indicating a shift ΔE_a of about 0.3 eV. This is in excellent agreement with the optical shifts ΔE_g of others^{1,8} and ours¹⁸ and, thus, with the simplest suggestion that ΔE_a has to do with a quantum confinement effect. This is also consistent, of course, with the fact that the excitonic Bohr radius of CdSe is 5.6 nm (Ref. 1) suggesting that the observed transition in $E_a(d)$ is also a signature of the transition to the weak confinement regime in CdSe.

Turning to the σ_0 values, we plot their dependence on E_a in Fig. 2. We see that, for very small E_a values (i.e., the large d values of the ZB phase), the σ_0 values (squares) are independent of d and that, for the mixed phase sample (triangle), the results are intermediate between those of the ZB samples and those of the HW samples (circles). The fact that there is no monotonic transition from the ZB to the HW behavior indicates that a simple semiconductor model (e.g., an increase in donor concentration, the dashed line) cannot account for the behavior presented by the solid line (also, see below). The interesting finding in Fig. 2, however, is that for the larger d values of the pure HW phase, we find a dependence (the solid line) that follows a very well-defined Meyer-Neldel rule (MNR).^{11,21–23} This dependence does not extend into the very small d samples (encircled dots) where there is a scatter of the $\log(\sigma_0)$ values. Noting that the optical gap E_g was found^{1,8} also to be changing through this latter d range of strong confinement, while σ_0 here does not, one can speculate that the transport character changes (e.g., from weaker to stronger coupling) as we go from the intermediate d (MNR-like behavior) regime to the strong confinement (small d) regime.

Returning to the MNR behavior (the solid line in Fig. 2), we further analyze the MNR dependence according to the relation^{11,21}

$$\log_e(\sigma_0) = \log_e(B_{\text{MNR}}) + E_d/E_{\text{MNR}}, \quad (2)$$

finding the MNR parameters $B_{\text{MNR}} = 4 \times 10^{-11} (\Omega \text{ cm})^{-1}$ and $E_{\text{MNR}} = 0.014 \text{ eV}$. These values show that the present system is remarkably different from that of, for example, hydrogenated amorphous silicon^{11,21} where, typically, $B_{\text{MNR}} = 6 \times 10^{-6} (\Omega \text{ cm})^{-1}$ and $E_{\text{MNR}} = 0.04 \text{ eV}$. The importance of this difference is that it shows that a very different mechanism controls the conduction process in each of the systems. In particular, the much smaller B_{MNR} in the case of CdSe nanocrystals suggests a conduction process with a lower probability than the one that is determined by extended states in disordered (amorphous) semiconductors. This, in turn, supports our previous suggestion¹⁹ of hopping conduction between the corresponding distributed quantum confinement shifted levels of adjacent crystallites rather than between defect and band-tail states in a disordered bulk material.

The above statistical shiftlike behavior appears, then, to be a clear indication of the increase of the separation between the conduction band edge E_c and E_F with decreasing d . This behavior can result, in principle, from either an increase of the band gap E_g while E_F is pinned, or from the rise of E_F due to an increase of the donor concentration with increasing d . While the above discussed former scenario that yields the MNR behavior is consistent with the optical data,^{1,8,18} the latter scenario is only consistent with an observed inverse MNR behavior²³ such as the one from the ZB to the HW doping-defect transition²⁴ (the dashed line in Fig. 2).

In trying to provide independent evidence for our interpretation of the above MNR in terms of a quantum confinement induced band shift, we studied the phototransport of the system. In Fig. 3, we show then the results of the measurements of the photoconductivity σ_{ph} and its light intensity exponent γ_e (defined by $\sigma_{\text{ph}} \propto G^{\gamma_e}$, where G is the photocarrier generation rate^{20,25,26}) that we measured as a function of E_d (i.e., of d). Two transitions in the d dependence of the mobility-lifetime product of the majority carriers (the electrons here) $(\mu\tau)_e (= \sigma_{\text{ph}}/qG$, where q is the elementary electronic charge) are clearly seen. These transitions take place *at the same d values* that we found for the transitions in the dark conductivity data. The results shown in Fig. 3(a) indicate that in the small d (strong confinement) regime, the dependence of $(\mu\tau)_e$ on d is the strongest, it weakens in the ‘‘intermediate confinement’’ regime, for which we found the MNR, and is practically nonexistent in the ZB regime. On the other hand, as seen in Fig. 3(b), the value of $\gamma_e(d)$ changes significantly only in this intermediate confinement regime. We do well know,^{25,26} from the simplest possible model of an n -type photoconductor, that for a single trapping-recombination level, E_t , a $\gamma_e \approx 0.5$ value is typical for an E_t that lies below E_F , while it reaches a $\gamma_e \approx 1$ value when E_t lies at (within a couple of kT 's) or above E_F . This is consistent with our model as follows. The observed behavior is known^{25,26} to result if E_F is relatively pinned and E_t is shifted upward through E_F (here with decreasing d , i.e., with

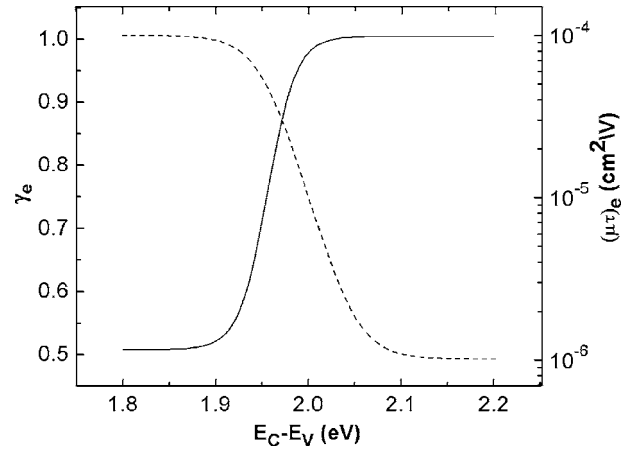


FIG. 4. The simulated dependence of the electron’s mobility-lifetime product (dashed curve) and the corresponding light intensity exponent (solid curve) on the bottom of the conduction band or the energy gap (i.e., on the crystallites size) in the corresponding CdSe quantum dots. The model used in the simulations is of a pinned Fermi energy and a single-level recombination center in a semiconductor which shifts simultaneously with the bottom of the conduction band. The band-gap range, $E_c - E_v$, considered here is typical of CdSe Qds (Refs. 1 and 8). The parameters used were $E_v = 0$, $E_c - E_i = 0.75 \text{ eV}$, $E_F = 1.1 \text{ eV}$, the density of states of both band edges was taken as $2.5 \times 10^{19} \text{ cm}^{-3}$, the concentration of the recombination centers was taken as 10^{17} cm^{-3} , and their capture coefficients for both electrons and holes was taken as $10^{-11} \text{ cm}^3 \text{ s}^{-1}$. The electron mobility value was taken as $1 \text{ cm}^2/\text{V s}$ and the temperature as 250 K .

increasing E_d). On the other hand, since the separation of E_c and E_t is determined by atomic forces, these two levels are expected to shift upward together with the decrease of d . This is in full accordance with our optical data¹⁸ and the expected quantum confinement. If, as above, we assume then that E_F is relatively pinned (with respect to the variations in d), the fact that $E_c = E_F + E_d$ implies that the $E_d(d)$ behavior is induced by the quantum confinement. Hence, our dark conductivity results, the observed optical shift of E_g and the $\gamma_e(d)$ behavior, are all consistent with the upward shift of E_c with decreasing d . It is important to note that the well-known difficulty of distinguishing between mobility and concentration variations, so typical for semiconductors, is removed in the evaluation of γ_e since this quantity depends only on the recombination kinetics and not on the transport mechanism.^{25,26}

To rigorously support the above scenario, we have conducted a comprehensive simulation study (such as in Ref. 20) of the effects of the relevant energy level shifts on the phototransport properties. Preferring simplicity to comprehensiveness in this presentation of our study (in particular, by leaving out mobility variation effects), we consider here only the very simple case of a pinned Fermi level with a single level of recombination centers E_t that (in contrast to all cases treated previously in the literature^{25,26}) shifts simultaneously with E_c . Indeed, the results we present in Fig. 4 clearly show the decrease of $(\mu\tau)_e$ and the increase of γ_e with the simultaneous upshift of E_c and E_t . These, in particular the behavior of γ_e , which depends solely^{25,26} on the po-

sitions of E_c , E_t , and E_F , are in full accordance with the expected increase of E_a (or $E_c - E_F$ or $E_c - E_t$, i.e., the band gap here) that we observed in Fig. 3. The increase of E_a with decreasing d , as shown in Fig. 1, associates then the behavior exhibited in Fig. 3 with the quantum confinement effect in the individual crystallites.

One should note, however, again, that, in principle, the results shown in Fig. 1 can be accounted for by a second scenario; i.e., that for some “unknown” reason there are more donorlike states with the increase of d , and thus the corresponding observed decrease of E_a with d has to do with a “pinned” E_c and an upshift of E_F . If this would have been the case, we should have that with increasing d there should also be a relative rise of E_F with respect to E_t and, thus, an *inverse* behavior to the one shown in Figs. 3 and 4 should have been observed, i.e., that γ_e should increase from $\frac{1}{2}$ to 1 (or stay at 1) and $(\mu\tau)_e$ should decrease with increasing d in contrast with our observations. Our comprehensive phototransport study shows, then, that the relative shift of the electronic levels with respect to a pinned (or relatively pinned) E_F is responsible for the various d dependencies that we found in this study. This, and the fact that the correspond-

ing variations of energy levels in the individual crystallites take place in the strong-to-intermediate quantum confinement regime ($8 < d \leq 11.2$ nm) of CdSe, provide, then, a clear evidence for the transport manifestation of the latter in solid-state ensembles of QDs.

In conclusion, we have shown that, in a solid ensemble of quantum dots, the macroscopic electrical properties reflect the quantum confinement effect in the individual crystallites. In particular, the behavior of the dark conductivity and the phototransport parameters were shown to result from band-gap broadening in the individual dots. In turn, the application of the concept of a macroscopic Fermi level to such ensembles is concluded to provide a very useful tool for the analysis and understanding of the transport in them. The transport parameters that we derived in this study also indicate, however, that the carrier propagation is determined by a low probability process that is associated with a relatively strong localization of the charge carriers in the quantum dots.

This work was supported in part by the Israel Science Foundation. I.B. is holding the Enrique Berman chair in Solar Energy Research at the HU.

-
- ¹S. V. Gaponenko, *Optical Properties of Semiconductor Nanocrystals* (Cambridge University Press, Cambridge, 1997).
- ²For recent reviews see *Semiconductor and Metal Nanocrystals*, edited by V. L. Klimov (Dekker, New York, 2004).
- ³U. Banin and A. Millo, *Annu. Rev. Phys. Chem.* **54**, 456 (2003).
- ⁴K. Walzer, E. Max, N. C. Greenham, and K. Stokbro, *Surf. Sci.* **532-535**, 795 (2003).
- ⁵D. S. Ginger and N. C. Greenham, *J. Appl. Phys.* **87**, 1361 (2000).
- ⁶C. B. Murray, C. R. Kagan, and M. G. Bawendi, *Science* **270**, 1335 (1995).
- ⁷C. R. Kagan, C. B. Murray, M. Nirmal, and M. G. Bawendi, *Phys. Rev. Lett.* **76**, 1517 (1996).
- ⁸M. V. Artemyev, A. I. Bibik, L. I. Gurionovich, S. V. Gaponenko, H. Jaschinskis, and U. Woggon, *Phys. Status Solidi B* **224**, 393 (2001), and references therein.
- ⁹See, for example, D. Yu, C. Wang, B. Wehrenberg, and P. Guyot-Sionnest, *Phys. Rev. Lett.* **92**, 216802 (2004).
- ¹⁰W. H. Lee, C. Lee, and J. Jang, *J. Non-Cryst. Solids* **198-200**, 911 (1996); E. Lampin, C. Delerue, M. Lannoo, and G. Allan, *Phys. Rev. B* **58**, 12044 (1998).
- ¹¹Y. Lubianiker and I. Balberg, *Phys. Rev. Lett.* **78**, 2433 (1997).
- ¹²M. Reshotko, I. Balberg, and A. Sa'ar, *Phys. Status Solidi A* **197**, 113 (2003), and references therein.
- ¹³B. Alpers, I. Robinstien, G. Hodes, D. Porath, and O. Millo, *Appl. Phys. Lett.* **75**, 1751 (1999), and references therein.
- ¹⁴S. K. Bera, S. Chaudhuri, R. P. Gupta, and A. K. Pal, *Thin Solid Films* **382**, 86 (2001).
- ¹⁵D. Nesheva, *J. Optoelectron. Adv. Mater.* **3**, 885 (2001).
- ¹⁶D. Pathinettam Padiyan, A. Marikani, and K. R. Murali, *Mater. Chem. Phys.* **78**, 51 (2002).
- ¹⁷S. S. Kale and C. D. Lokhande, *Mater. Chem. Phys.* **62**, 103 (2000); E. U. Masumdar, V. B. Gaikwad, V. B. Pujari, P. D. More, and L. P. Deshmukh, *ibid.* **77**, 669 (2002).
- ¹⁸A. Rivera-Marquez, M. Rubin-Falfan, R. Lozada-Morales, O. Pottillo-Moreno, O. Zelaya-Angel, J. Luyo-Alvarado, M. Melendez-Lira, and L. Banos, *Phys. Status Solidi A* **188**, 1059 (2001), and references therein.
- ¹⁹D. Toker, I. Balberg, O. Zelaya-Angel, E. Savir, and O. Millo, *Phys. Rev. B* **73**, 045317 (2006).
- ²⁰I. Balberg, Y. Dover, R. Naides, J. P. Conde, and V. Chu, *Phys. Rev. B* **69**, 035203 (2004).
- ²¹H. Overhof and P. Thomas, *Electronic Transport in Hydrogenated Amorphous Semiconductors* (Springer-Verlag, Berlin, 1989).
- ²²A. Yelon, B. Movaghar, and H. M. Branz, *Phys. Rev. B* **46**, 12244 (1992).
- ²³G. Lucovsky and H. Overhof, *J. Non-Cryst. Solids* **164-166**, 973 (1993).
- ²⁴A. O. Oduor and R. D. Gould, *Thin Solid Films* **270**, 387 (1995).
- ²⁵R. H. Bube, *Photoelectronic Properties of Semiconductors* (Cambridge University Press, Cambridge, 1992).
- ²⁶I. Balberg, *J. Appl. Phys.* **75**, 914 (1994).